Genetic attributes of cerebrospinal fluid-derived HIV-1 *env*

Satish K. Pillai,[1,2,4] Sergei L. Kosakovsky Pond,[1] Yang Liu,[5] Benjamin M. Good,[1,3] Matthew C. Strain,[1] Ronald J. Ellis,[1,6] Scott Letendre,[1,6] Davey M. Smith,[1,3] Huldrych F. Günthard,[7] Igor Grant,[1,6] Thomas D. Marcotte,[1,6] J. Allen McCutchan,[1,6] Douglas D. Richman[1,3] and Joseph K. Wong[1,2,4]

[1]University of California, San Diego, La Jolla, [2]University of California, San Francisco, San Francisco, [3]VA San Diego Healthcare System, San Diego, [4]VA Medical Center San Francisco, San Francisco, [5]Monogram Biosciences, Inc., South San Francisco, [6]HIV Neurobehavioral Research Center, San Diego, CA, USA; and [7]Division of Infectious Diseases and Hospital Epidemiology, University Hospital Zurich, Zurich, Switzerland

Correspondence to: Satish K. Pillai, UCSF Department of Medicine/NCIRE, 4150 Clement Street (111W3), San Francisco, CA 94121, USA
E-mail: satish.pillai@ucsf.edu

HIV-1 often invades the CNS during primary infection, eventually resulting in neurological disorders in up to 50% of untreated patients. The CNS is a distinct viral reservoir, differing from peripheral tissues in immunological surveillance, target cell characteristics and antiretroviral penetration. Neurotropic HIV-1 likely develops distinct genotypic characteristics in response to this unique selective environment. We sought to catalogue the genetic features of CNS-derived HIV-1 by analysing 456 clonal RNA sequences of the C2-V3 *env* subregion generated from CSF and plasma of 18 chronically infected individuals. Neuropsychological performance of all subjects was evaluated and summarized as a global deficit score. A battery of phylogenetic, statistical and machine learning tools was applied to these data to identify genetic features associated with HIV-1 neurotropism and neurovirulence. Eleven of 18 individuals exhibited significant viral compartmentalization between blood and CSF ($P < 0.01$, Slatkin–Maddison test). A CSF-specific genetic signature was identified, comprising positions 9, 13 and 19 of the V3 loop. The residue at position 5 of the V3 loop was highly correlated with neurocognitive deficit ($P < 0.0025$, Fisher's exact test). Antibody-mediated HIV-1 neutralizing activity was significantly reduced in CSF with respect to autologous blood plasma ($P < 0.042$, Student's *t*-test). Accordingly, CSF-derived sequences exhibited constrained diversity and contained fewer glycosylated and positively selected sites. Our results suggest that there are several genetic features that distinguish CSF- and plasma-derived HIV-1 populations, probably reflecting altered cellular entry requirements and decreased immune pressure in the CNS. Furthermore, neurological impairment may be influenced by mutations within the viral V3 loop sequence.

Introduction

HIV-1 and simian immunodeficiency virus (SIV) cross the blood–brain barrier during primary infection, eventually resulting in neurological complications in up to 50% of untreated individuals (Ho *et al.*, 1985; Grant *et al.*, 1987; Heaton *et al.*, 1995; Price, 1996; Zink *et al.*, 1999; Pierson *et al.*, 2000; Clements *et al.*, 2002). HIV-associated dementia, encephalopathy and sensory neuropathies contribute significantly to morbidity and mortality (McArthur *et al.*, 2003). In addition, the CNS may serve as a sanctuary site for long-term viral persistence due to the suboptimal

penetration of several antiretroviral agents (Misra *et al.*, 2003).

The CNS is a distinct viral reservoir, differing from peripheral tissues in immunological surveillance, cytokine milieu, target cell characteristics and antiretroviral penetration. Evidence from humans and chimpanzees suggests that selective pressure from anti-HIV neutralizing antibodies and cytotoxic T cells may be diminished in the brain and CSF (Goudsmit *et al.*, 1987; Ljunggren *et al.*, 1989; von Gegerfelt *et al.*, 1992; Ruta *et al.*, 1998; Pachter *et al.*, 2003; Song *et al.*, 2004). Cytokines such as CXCL12, interleukin-6, tumour necrosis factor-alpha and RANTES that modulate HIV replication may differ in relative concentrations between the CSF and blood plasma (Gonzalez-Scarano and Martin-Garcia, 2005). The predominant targets of HIV-1 infection in the CNS are brain-derived macrophages and microglial cells, rather than the $CD4^+$ lymphocytes that serve as targets in the periphery (Gartner *et al.*, 1986). Several antiretroviral drugs do not efficiently cross the blood–brain barrier, possibly limiting the suppression of viral replication in the CNS (Staprans *et al.*, 1999; Misra *et al.*, 2003).

The uniqueness of the CNS environment is often reflected in compartment-specific HIV-1 genotypic and phenotypic characteristics. Contemporaneous CNS- and blood-derived viruses are frequently compartmentalized on the basis of phylogenetic analysis of intrapatient sequences (Korber *et al.*, 1994; Power *et al.*, 1995; Hughes *et al.*, 1997; Wong *et al.*, 1997; Gorry *et al.*, 2001; Ohagen *et al.*, 2003; Strain *et al.*, 2005; McCrossan *et al.*, 2006), and brain-derived *env* sequences may share signature mutations across individuals (Korber *et al.*, 1994; Power *et al.*, 1994). Differences in CD4 dependence, co-receptor usage phenotype and LTR sequence have been observed between brain- and blood-derived HIV isolates, reflecting differences in chemokine receptor expression and transcriptional environment between microglia and peripheral host cells (Shieh *et al.*, 1998; Ross *et al.*, 2001; Argyris *et al.*, 2003; Hogan *et al.*, 2003; Zhou *et al.*, 2003; Burdo *et al.*, 2004). The presence of discordant drug-resistance mutations in CSF and plasma viral populations probably results from tissue-specific variation in drug efficacies due to the poor penetration of certain antiretroviral agents (Wong *et al.*, 1997; Cunningham *et al.*, 2000; Venturi *et al.*, 2000; Cinque *et al.*, 2003; Strain *et al.*, 2005). Moreover, recent evidence suggests that the evolution of resistance may differ between brain subcompartments (Smit *et al.*, 2004).

HIV-1 RNA is detectable in the CSF of most infected individuals throughout disease. Owing to the obvious sampling difficulties associated with brain tissue, CSF virus has often been investigated as a proxy for brain-derived HIV-1 (studies of brain virus are almost exclusively limited to post-mortem samples). This indirect sampling strategy is supported by phylogenetic evidence that CSF and brain-derived viral populations are more closely related to each other than with populations derived from bone marrow, kidney, liver, lung, lymph nodes and spleen (Sanjuan *et al.*,

2004). We previously described a high frequency of discordant patterns of HIV drug resistance and partitioning of C2-V3 *env* sequences from 18 matched CSF and plasma samples (Strain *et al.*, 2005). Here, we performed a more detailed analysis of these clonal sequences to catalog the genetic and evolutionary features that distinguish CSF- and blood plasma-derived HIV-1 populations. In addition, the extent of HIV neutralizing activity conferred by CSF and plasma from five chronically infected individuals within this cohort was measured using an *in vitro* assay to compare and contrast the immunological conditions in these two tissue compartments. Finally, we investigated the genetic basis of neurovirulence by comparing CSF-derived sequences from several individuals with known global deficit scores (GDS) based on a comprehensive neuropsychological evaluation. Our analysis suggests that HIV-1 neurotropism and neurovirulence in chronically infected individuals are modulated by residues in and around the V3 loop subregion of the viral envelope, and, moreover, attenuated immune surveillance in the CNS may contribute to the discordant evolutionary patterns observed in CSF- and plasma-derived HIV-1 populations.

(Presented in part at the 6th International Symposium on Neurovirology, Sardinia, Italy, September 2004.)

Material and methods
Subjects
Twenty-one individuals enrolled in clinical studies at the HIV Neurobehavioral Research Center (HNRC) between 1998 and 2002 were initially examined. All subjects had stable or no antiviral therapy for at least 2 months before the study, had plasma and CSF HIV RNA of >500 copies/ml and had no evidence of systemic or CNS opportunistic infections or malignancy based on clinical, laboratory and/or neuroimaging studies. Data were available on past and present therapy, current HIV RNA and CD4 counts, nadir CD4 counts and CSF cell counts (Table 1). All studies were conducted in compliance with local institutional review board (IRB) guidelines and with subjects' written informed consent.

Specimen processing
Paired blood from peripheral venipuncture in acid citrate dextrose (ACD) tubes and CSF from lumbar punctures were collected (typically collected within 1 h of each other) and processed within 2 h of collection. Plasma and cell-free CSF were aliquoted, frozen and stored at -70°C until processing. All subsequent plasma and CSF processing was performed separately to minimize the within-subject cross-contamination of samples.

Nucleotide sequencing
Sequencing methods were previously described in full (Strain *et al.*, 2005). In brief, reverse transcription and polymerase chain reaction (PCR) amplification of C2-V3 *env* for each sample was performed in triplicate or quadruplicate using the Finnzyme one-step RT–PCR kit (MJ Research, Waltham, MA, USA) and primers V3Fout and V3Bout as described previously in a 25 μl reaction volume. About 2.5 μl of first-step RT–PCR product was used in the second, nested PCR reaction with primers V3Fin and V3Bin (Strain *et al.*, 2005).

Table 1 Subject characteristics

Patient	CSF HIV-1 RNA (log copies/ml)	Plasma HIV-1 RNA (log copies/ml)	Current CD4 (cells/mm^3)	Nadir CD4 (cells/mm^3)	NP GDS	Any Rx	Current Rx
A	4.5	4.9	355	133	1.28	+	−
B	5.2	5.5	219	112	2.13	+	+
C	5.2	5.7	312	312	0.44	−	−
D	4	5.9	55	23	0.69	+	−
E	4	4.7	277	277	1.41	+	−
F	4.8	4.7	688	391	0.88	+	+
H	4.3	4.9	267	248	0.53	+	−
I	4.6	6	112	112	NA	+	−
J	6.2	5.2	153	153	0.75	−	−
K	4.4	5.7	221	221	0.5	−	−
L	3.2	6	32	10	0.63	+	+
M	3.8	5.2	91	91	0.56	+	+
N	4.6	4.5	145	145	0.31	+	+
O	3.3	5.6	43	30	1.4	−	−
P	3.2	5.9	60	56	1.18	+	−
Q	3.5	5.1	68	68	0.94	+	−
R	2.9	5.1	16	16	3.5	+	+
S	3.2	6	32	32	2.88	+	−
Median	4.15	5.35	128.5	112	0.88		

NA = not available; any Rx = past or present antiretroviral therapy; current Rx = on antiretroviral therapy at time of sampling or within 2 months of sampling (adapted from Strain et al., 2005).

All assays included negative controls and were conducted in conditions to minimize the potential for PCR contamination utilizing aerosol-resistant pipet tips, dedicated PCR reagents and laminar flow hoods. Replicate PCR products were proportionately pooled and cloned using the TOPO-TA cloning system (Invitrogen, Carlsbad, CA, USA). Purified plasmids were sequenced in both directions with −20M13 primer (5′-gtaaaacgacggccag-3′) and Topo Forward primer (5′-tggatatctgcagaattcg-3′) using Prism Dye terminator kits (ABI, Foster City, CA, USA) on an ABI 3100 Genetic Analyzer. Sequences were compiled, aligned and edited using Sequencher 4.0 (Genecodes, Ann Arbor, MI, USA) and Clustal (version 1.81).

Neuropsychological assessment

Subjects completed a detailed neuropsychological assessment measuring their functioning in eight cognitive ability domains: verbal functioning, abstraction, complex perceptual-motor skills, attention, learning, memory, motor skills and sensory functioning. Test results were summarized as 'deficit scores', which reflect the number and severity of impaired performances throughout the test battery and give relatively less weight to test performances within or above the average range. A GDS is computed by adding the deficit ratings of the component test measures and dividing by the total number of measures. Deficit scores are sensitive to the presence and pattern of NP impairments in HIV+ individuals (Heaton et al., 1995). Statistical classification of NP impaired/NP normal was made through the use of a GDS cut-off score that demonstrates high accuracy in predicting clinician ratings of NP status. A GDS of 0.5 or greater is considered to be in the impaired range. This represents at least mild impairment on half of the tests of the NP battery (Carey et al., 2004).

Phylogenetic reconstruction

Initial multiple sequence alignments were generated using ClustalX (Thompson et al., 1994), with default gap parameters and the 'IUB' DNA weight matrix. Subsequent manual aligning was performed using the Se–Al sequence alignment editor (Rambaut, 1996; http://evolve.zoo.ox.ac.uk/). Phylogenies describing sequences from each individual host were built using FastDNAml (Olsen et al., 1994), estimating base frequencies from the data, Ts/Tv ratio of 2.0. Diversity measurements were calculated using dnadist and protdist (Felsenstein, 1993). A master tree describing the entire data set was built by implementing dnadist and neighbor within the Phylip 3.5c package (Felsenstein, 1993) using the F84 model, gamma distributed rates across sites and Ts/Tv ratio of 2.0. Trees were viewed using TreeView X (Page, 1996).

Evaluation of compartmentalization

The degree of segregation between compartments was assessed by testing for panmixis using gene phylogenies (Slatkin and Maddison, 1989; Hudson et al., 1992) as implemented in MacClade (Sinauer, Sunderland, MA, USA). In brief, the minimum possible number of inter-compartment migration events was tallied, on the basis of the maximum likelihood trees for each individual subject's C2-V3 sequences and their characterization according to compartment of origin. This result was compared with the distribution of migration events in 1000 trees in which the taxa have been randomly shuffled across tips, retaining the original topology and associated polytomies (Nickle et al., 2003b). Evidence of restricted gene flow (compartmentalization) was documented when <1% of the randomized trees required the same or a fewer number of migration events as for the sample data (Slatkin and Maddison, 1989).

Machine learning classification

All classification experiments in this analysis were conducted using WEKA (Waikato Environment for Knowledge Analysis), an open-source collection of data processing and machine learning algorithms (Witten and Frank, 2000). The J48 decision tree inducer, based on the C4.5 algorithm (Quinlan, 1993), was implemented with the parameter 'MinNumObj' set at a value of 11 to limit the complexity of theories and minimize the risk of over-fitting. Classifiers were evaluated using 100 iterations of stratified 10-fold cross-validation, a procedure designed to conservatively reflect the performance of classification models on novel data sets (Witten and Frank, 2000).

Analysis of selection

We used a procedure described by Leigh Brown *et al.* (A. J. Leigh Brown, S. L. Kosakovsky Pond, Z. Grossman, D. D. Richman, S. D. Frost, submitted for publication) to test for differential selective pressure on a given codon in two populations. First, branch lengths and nucleotide substitution biases under an appropriate nucleotide substitution model are inferred from the entire alignment. Secondly, holding these parameters constant, a version of the MG94xREV codon model (http://mbe.oxfordjournals.org/cgi/content/abstract/msi232v1) is used to estimate synonymous (α_s) and non-synonymous substitution rates (β_s^L) at each codon s independently in sequences from two different populations. We say that differential evolution has acted on codon s when $\omega_s = \beta_s/\alpha_s$ differs significantly between two populations. Formally,

$$H_0 : \beta_s^1 = R\alpha_s^1 \text{ and } \beta_s^2 = R\alpha_s^2 \quad \text{No differential evolution}$$
$$H_A : \beta_s^1, \alpha_s^1, \beta_s^2, \alpha_s^2 \qquad\qquad \text{Differential evolution}$$

Significance of the difference can be assessed by assuming the χ_1^2 distribution for the likelihood ratio. This test is conservative, but has a high positive predictive value (>95%) based on simulated data (Kosakovsky Pond and Frost, 2005; A. J. Leigh Brown, S. L. Kosakovsky Pond, Z. Grossman, D. D. Richman, S. D. Frost, submitted for publication).

Analysis of glycosylation

GlycoTracker.pl (S. K. Pillai, unpublished data) was used to identify N-linked glycosylation sites within each sequence. The perl script provides a tally of all glycosylation sites, along with their respective locations (numbered according to HXB2 gp160). We compared the extent and distribution of N-linked glycosylation across the C2-V3 region in both compartments by identifying 'N[X]S' and 'N[X]T' motifs in plasma- and CSF-derived sequences (Marshall, 1974).

Neutralization assay

Antibody-mediated neutralization of HIV-1 was measured using a previously described recombinant virus assay (Richman *et al.*, 2003). Neutralizing activity present in plasma was compared with that in CSF against prototypic lymphocytotropic (NL4-3) (Adachi *et al.*, 1986) and macrophage-tropic (JR-CSF) (Koyanagi *et al.*, 1987) HIV strains. Standardized inocula of recombinant, luciferase expressing viral constructs pseudotyped with NL4-3 or JR-CSF Env were incubated with serial dilutions of either CSF or plasma collected from the same time point. Infection of U87 cells transduced to express CD4/CXCR4/CCR5 yields a luminescent read-out that is inversely proportional to the neutralizing activity

in the study fluid. To exclude non-neutralizing antibody-mediated inhibition by other substances such as antiviral drugs, parallel experiments were performed with ampho-MuLV pseudotyped virus as described previously (Richman *et al.*, 2003).

Survey of publicly available sequence data

All available CSF-derived subtype B V3 loop sequences with accompanying patient identification information were downloaded from the Los Alamos National Lab HIV Sequence Database. A majority-rule consensus sequence was generated for each patient's sequence data. CSF-derived consensus sequences were compared against all available peripheral V3 loop sequences in the Los Alamos subtype B web alignment (which contains one single representative sequence per patient).

Statistical analysis

The following non-parametric tests were applied to these data, as implemented in JMP version 5.1 (SAS Institute, Cary, NC, USA): Mann–Whitney *U*-test, Wilcoxon signed-rank test and Fisher's exact test.

Nucleotide sequence accession numbers

The C2-V3 *env* sequences were submitted to GenBank and assigned accession numbers DQ143360 to DQ143815.

Results

Compartmentalization of CSF-derived virus

Nucleotide sequences representing CSF- and plasma-derived viruses were successfully generated for 18 out of 21 individuals initially enrolled in this study (Table 1). A total of 456 clonal CSF and plasma *env* sequences were generated and analysed to determine the genetic characteristics of CSF-derived HIV-1. We evaluated the compartmentalization of contemporaneous CSF- and plasma-derived sequences by applying a modified version of the parsimony-based cladistic method of Slatkin and Maddison (1989) to maximum likelihood phylogenetic reconstructions (Nickle *et al.*, 2003*a*, *b*). According to this stringent test of panmixis, 11 of 18 individuals (individuals A, F, H, J, M-S) in this cohort exhibited independent clustering of tissue-specific populations ($P < 0.01$), while 2 of the remaining 7 individuals (B, L) harboured variants that exhibited partial compartmentalization between tissues ($0.01 < P < 0.05$) (Fig. 1).

Amino acid diversity in plasma- and CSF-derived viral populations

We next calculated the amino acid diversity of C2-V3 sequences from CSF and plasma, focusing on average pairwise distances derived using the Dayhoff PAM substitution matrix (Dayhoff *et al.*, 1978). There was no significant difference in overall protein diversity between CSF- and plasma-derived sequences pooled across all 18 individuals (data not shown). When focusing exclusively on the V3 loop subregion, however, there was a significant reduction
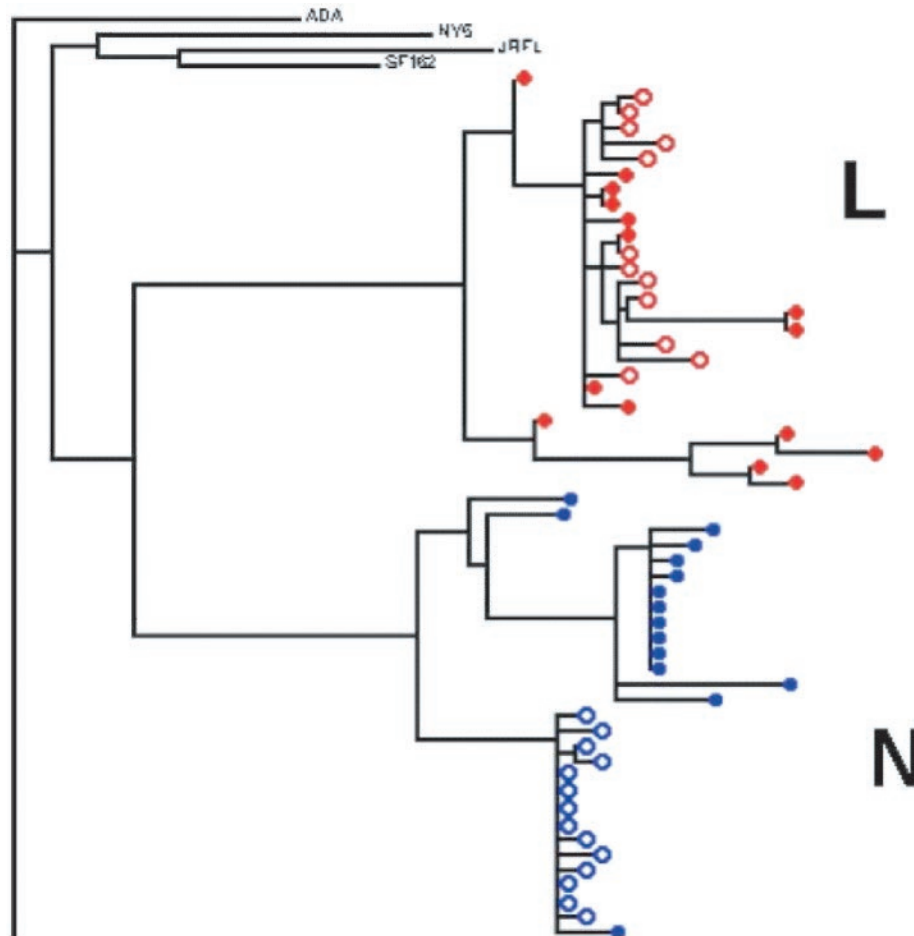
Fig. 1 Examples of compartmentalized and non-compartmentalized viral populations. Maximum likelihood phylogenies of C2-V3 *env* sequences. Red circles = individual L (non-compartmentalized virus), and blue circles = individual N (compartmentalized virus). Open circles represent CSF sequences, and closed circles indicate plasma-derived sequences. Strains ADA, NY5, JRFL and SF162 included as outgroups.

of diversity in CSF-derived sequences ($P < 0.05$, Wilcoxon signed rank) (Fig. 2). Tissue-specific patterns of diversity did not differ between compartmentalized and non-compartmentalized individuals.

CSF-specific Env genetic signature

CSF-derived viruses may share genetic characteristics across individuals due to tissue-specific selective pressures that are common across hosts. We employed a previously described machine learning approach to look for evidence of a genetic signature shared by CSF-derived sequences pooled across individuals (Pillai *et al.*, 2005). The training data for this experiment drew samples from the entire available sequence set, consisting of 231 plasma sequences and 225 from CSF. Our results (data not shown) indicated that there was no evidence of a signature, on the basis of the high error rate associated with the classification trial; tissue tropism was misclassified in nearly 50% of test cases. However, when we limited our analysis to the 94 plasma and 130 CSF sequences associated with the 11 compartmentalized individuals (A, F, H, J, M-S), classification accuracy

(conservatively estimated using a cross-validation procedure) increased dramatically to 87%. The genetic signature underlying the classification model consisted of positions 5, 9, 13 and 19 of the V3 loop (HXB2 gp160 positions 300, 304, 308 and 314, respectively) (Supplementary Fig. 1). The presence of proline or histidine at V3 loop position 13 (gp160 position 308) was significantly correlated with compartmentalization in the CSF ($P < 0.044$, Fisher's exact test). In addition, the highest net difference in site-specific variability between CSF and plasma (as measured by Shannon entropy) was observed at V3 loop position 13 (Supplementary Fig. 2). Compartmental differences in relative amino acid composition at these signature sites are evident in Env alignments of each individual's sequences (Supplementary Fig. 3) and in (pooled) consensus sequence logos (Fig. 3). To assess whether the signatures identified here could be generalized to independent data sets, we performed a survey of publicly available subtype B sequences in the Los Alamos HIV Sequence Database. This analysis supported our earlier observations; the frequency of histidine or proline at position 13 of the V3 loop was significantly higher in CSF-derived
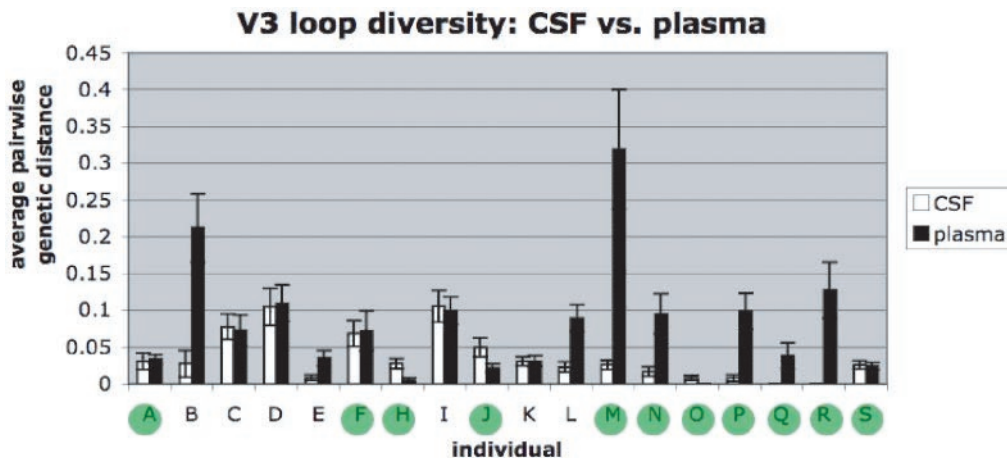
Fig. 2 V3 amino acid diversity in CSF- and blood-derived viral populations. Diversity was significantly lower in CSF-derived viral populations across individuals ($P < 0.01$, Wilcoxon test). Green circles indicate compartmentalized individuals. Vertical bars represent standard error.
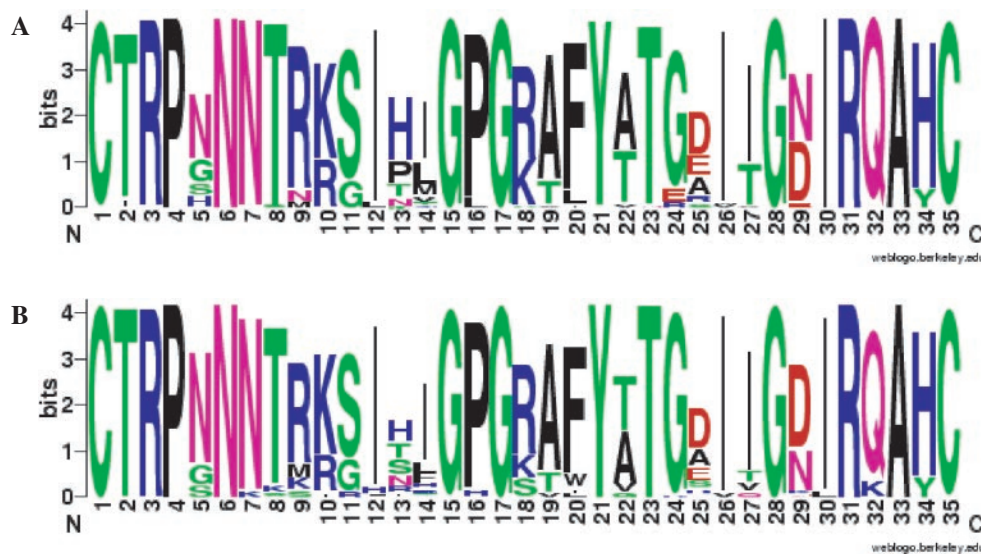

Fig. 3 Consensus V3 loop sequences of (**A**) CSF and (**B**) plasma. The overall height of each position is proportional to its conservation. Relative height of each amino acid reflects its prevalence at that site. The prevalence of proline and histidine at position 13 is significantly higher in CSF sequences.

sequences ($P < 0.048$, Fisher's exact test). CSF-derived consensus sequences from 75% of patients (21 of 28) with available CSF sequence data contained either histidine or proline at position 13. Conversely, only 56.5% of peripheral sequences (100 of 177) contained either of these residues at position 13 (data not shown).

Identification of discordantly selected sites

We used a maximum likelihood approach to identify codons within *env* that were under discordant selection pressure in CSF and plasma. Selection pressure is described as the ratio between non-synonymous substitutions per non-synonymous site (dN) and synonymous substitutions per synonymous site (dS) (Nei and Gojobori, 1986). A total of seven sites in the C2-V3 region exhibited discordant

levels of selection pressure (dN/dS) in CSF and plasma, based on a differential *P*-value cut-off of 0.1 (Table 2). Five out of these seven sites were under strong negative selection in CSF while corresponding sites were under positive selection or evolving neutrally in blood plasma (Table 2). These data are in alignment with our compartment-specific maximum likelihood estimates of global dN/dS across the C2-V3 region. CSF-derived HIV-1 sequences exhibited considerably lower dN/dS values than plasma-derived sequences (data not shown).

N-linked glycosylation in plasma- and CSF-derived viral populations

We next examined N-linked glycosylation patterns across the C2-V3 *env* subregion, which are believed to vary in

Table 2 Sites within *env* C2-V3 under differential selective pressure in plasma and CSF

| HXB2 *env* position	CSF (dN/dS)	Plasma (dN/dS)	Differential *P*-value	Transition type
249	0.0000/1.5313	0.1499/0.0000	0.0923	Negative→neutral
250	0.0000/0.8244	0.1313/0.0000	0.0947	Negative→neutral
251	0.2539/0.0000	0.0000/1.3152	0.0499	Neutral→negative
255	0.0000/2.0299	0.4633/1.6224	0.0795	Negative→neutral
286	0.0000/0.8520	1.1051/0.0000	0.0131	Negative→positive
330	0.0000/3.2736	0.3629/0.9094	0.0694	Negative→neutral
346	1.5486/0.0000	0.9555/0.4798	0.092	Positive→neutral
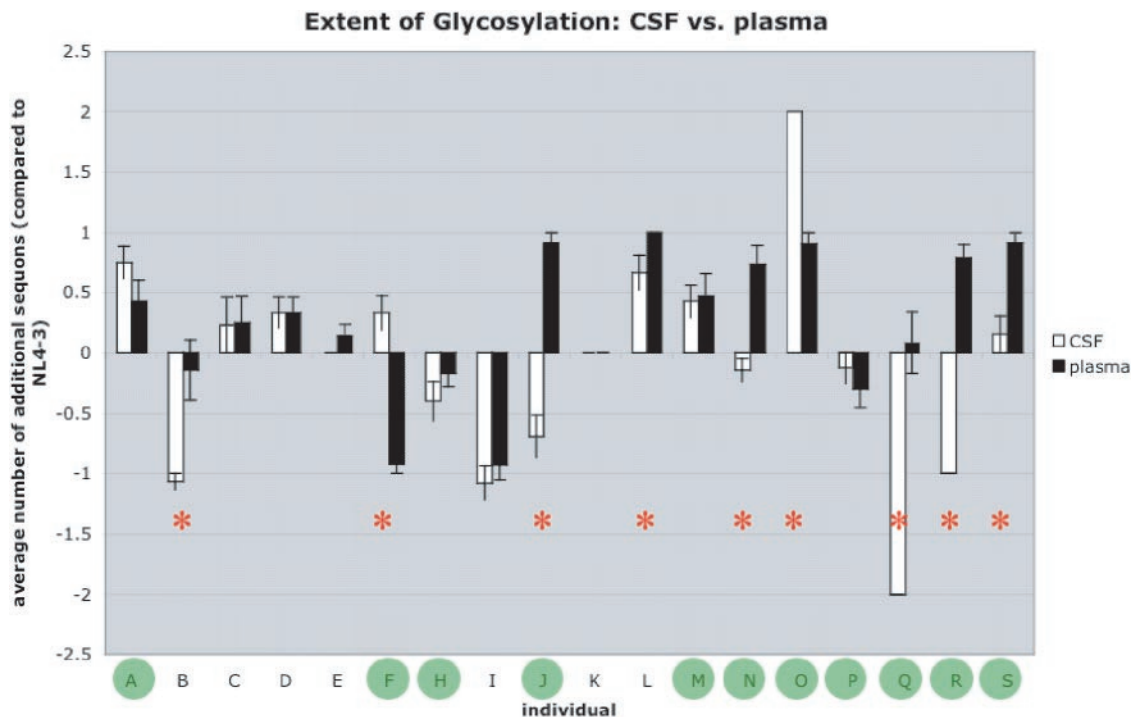
Fig. 4 Extent of glycosylation (number of N-linked glycosylation sites) in CSF- and plasma-derived C2-V3 sequences. Green circles indicate compartmentalized individuals. Red asterisks indicate significant differences between compartments (*P* < 0.05, Mann–Whitney). Whisker bars represent standard error. Seven out of 11 compartmentalized individuals have significantly different numbers of glycosylation sites in CSF- and plasma-derived sequences, and 5 out of those 7 have greater numbers in plasma populations.

response to selection pressure from the neutralizing antibody response (Wei *et al.*, 2003; Derdeyn *et al.*, 2004; Chohan *et al.*, 2005). Our analysis revealed that extent of glycosylation, reported as average number of glycosylation sites (sequons) per sequence, tended to be lower in CSF-derived viruses, although this trend was not quite significant (*P* < 0.062, Wilcoxon signed rank) (Fig. 4). Virus from 7 out of 11 compartmentalized individuals exhibited significantly different levels of glycosylation between compartments (*P* < 0.05, Mann–Whitney), and 5 out of these 7 had lower numbers of sequons in CSF-derived sequences (Fig. 4).

Antibody-mediated neutralization of HIV-1 by CSF and plasma

The HIV-1 neutralizing activity of CSF and plasma was measured to evaluate the hypothesis that reduced glycosylation of CSF-derived viruses resulted from attenuated local immune surveillance. This exploratory data involved six individuals in our cohort (B, H, J, M, N, and O), selected on the basis of discordant tissue-specific glycosylation patterns and availability of specimens to perform the neutralization assays. Neutralizing activity against HIV-1 NL4-3 and JR-CSF was measured using a previously described recombinant virus assay (Richman *et al.*, 2003). Data associated with individual B were excluded from analysis owing to non-specific neutralizing activity of residual antiretroviral drug in the plasma (data not shown). In all cases, antibody-mediated neutralization of HIV-1 was significantly greater in blood plasma (*P* < 0.042, Student's *t*-test), in accordance with the viral glycosylation data (Fig. 5). Neutralizing activity in CSF was below the background of detection in the majority of cases.
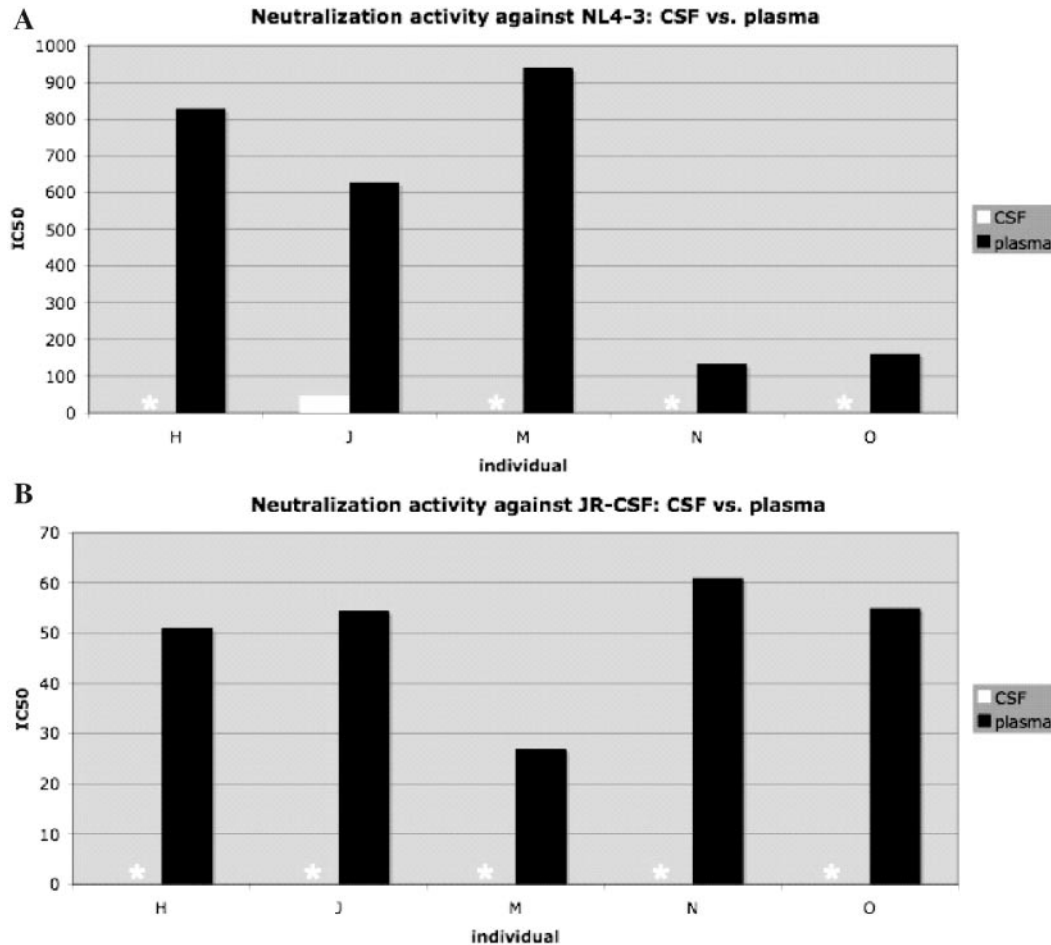
Fig. 5 Neutralization activity in CSF and plasma against prototypic lymphocytotropic and macrophage-tropic HIV-1 strains. (**A**) Neutralization activity against NL4-3, (**B**) neutralization activity against JR-CSF. Asterisks indicate responses below the assay's limit of detection. No significant neutralization of AMV Env pseudotyped virus was seen for these patients' sera, verifying that these responses are against HIV env (data not shown).

Correlation between *env* sequence and neurovirulence

All of the subjects involved in this study underwent a comprehensive neuropsychological assessment measuring their functioning in a variety of cognitive ability domains. Test results were summarized as 'deficit scores', which reflect the number and severity of impaired performances throughout the test battery. GDS in this cohort ranged from 0.31 (normal) to 3.5 (moderate to severe impairment) (Table 3). We looked for correlations between HIV-1 *env* sequence and cognitive deficit scores using machine learning-based regression analysis. The residue at position 5 of the V3 loop (HXB2 gp160 position 300) was the strongest predictor of GDS. Specifically, the presence of serine at position 5 was significantly correlated with topmost quartile GDS ($P < 0.0025$, Fisher's exact test) (Table 3).

Discussion

The results of our investigation reveal that the genetics of CSF- and blood plasma-derived strains of HIV-1 differ on

several levels, confirming previous reports that HIV-1 within the CNS can differ from virus in peripheral tissues. This study extends those observations by cataloguing the CSF-specific population genetic features of the HIV-1 quasi-species. First, the CNS (as represented by CSF) functions as a viral compartment in most, but not all, infected individuals. Secondly, sequence diversity of the V3 loop *env* subregion measured at the amino acid level is reduced in CSF-derived viral populations. Thirdly, there is a CSF-specific HIV-1 genetic signature associated with sequences from compartmentalized individuals comprising four sites within the V3 loop region. Fourth, several sites in the viral envelope are under different levels of selective constraint in CSF and plasma, and exhibit discordant levels of entropy in these tissues. Lastly, CSF-derived viruses tend to be less glycosylated than blood-derived viruses, probably reflecting the near lack of HIV neutralizing activity in CSF.

Viral compartments are characterized by a restriction of gene flow between cells or tissues, usually identified by phylogenetic analysis (Nickle *et al.*, 2003*a*; Pillai *et al.*, 2005). If

Table 3 Relationship between degree of cognitive deficit and consensus residue at position 5 of the V3 loop in CSF- and plasma-derived sequences

Individual	p5-CSF	p5-plasma	GDS
R	S	S	3.5
S	H	N	2.88
B	S	S	2.13
E	S	S	1.41
O	S	N	1.4
A	N	N	1.28
P	N	N	1.18
Q	N	N	0.94
F	N	N	0.88
J	N	N	0.75
D	N	N	0.69
L	N	N	0.63
M	N	N	0.56
H	G	G	0.53
K	N	N	0.5
C	N	N	0.44
N	G	G	0.31

GDS = global deficit score. Individuals listed from highest to lowest cognitive deficit.

the CSF represents a distinct viral compartment, contemporaneous CSF- and plasma-derived sequences are expected to cluster independently in a phylogenetic tree. We previously looked for evidence of compartmentalization between CSF and blood plasma (Strain *et al.*, 2005) by applying the parsimony-based cladistic method of Slatkin and Maddison (1989) to phylogenetic reconstructions. Inter-population gene flow may be underestimated by this approach, however, owing to the potential loss of polytomies in the randomly generated trees used to evaluate statistical significance (Nickle *et al.*, 2003*a*). We circumvented this issue by modifying the Slatkin–Maddison test; we generated 1000 random trees in which the taxa have been randomly shuffled across tips, retaining the original topology and associated polytomies. The results of this more conservative test of panmixis did not conflict with our original findings. Viral compartmentalization between blood and the CNS was identified in 13 out of 18 individuals. Viral migration across the blood–brain barrier was minimal and infrequent in these individuals, which reinforces the concept that a significant fraction of virus sampled in CSF is produced locally in the CNS (Sanjuan *et al.*, 2004). We looked for a clinical predictor of HIV-1 compartmentalization (e.g. current CD4 count), but failed to find any significant correlations, perhaps owing to limited sample size. Two comparisons were on the verge of significance, however; drug treatment and high CSF viral load ($>10^4$ copies/ml) were associated with phylogenetic partitioning of *env* sequences ($P < 0.09$, and $P < 0.10$, respectively; Fisher's exact test).

CSF-derived V3 loop sequences were under stronger negative selection and exhibited reduced levels of amino acid diversity in comparison with blood-derived sequences. These genetic characteristics probably reflect constraints associated with tissue-specific cellular entry determinants and reduced immune selection pressure in the CNS (Shieh *et al.*, 1998; Argyris *et al.*, 2003; Pachter *et al.*, 2003). A low viral effective population size in the CNS may contribute to the reduced diversity as well (Leigh Brown, 1997), although potential sampling effects resulting from lower CSF RNA copy numbers cannot be entirely excluded. Tissue-specific cellular entry may be influenced by HIV-1 co-receptor usage phenotype, which is largely determined by the amino acid sequence and net charge of the V3 loop (Pillai *et al.*, 2003). We computed net charge and predicted the co-receptor usage phenotype of these viruses using a machine learning algorithm (Pillai *et al.*, 2003), but did not observe any correlation between tissue of origin and co-receptor preference; CCR5 usage was nearly universal across compartments and individuals (data not shown, *see* Supplementary Fig. 4). To pursue the reduced immune selection hypothesis, we examined the N-linked glycosylation patterns across the C2-V3 *env* subregion and measured the HIV-1 neutralizing activity of CSF and plasma using an *in vitro* assay. The observed trend towards reduced glycosylation in CSF-derived viral sequences and near lack of neutralizing activity in the CSF of our exploratory group of six individuals offers strong support to the hypothesis that reduced immune surveillance plays an important role in driving the independent evolution of HIV-1 in the CNS.

The identification of a CSF-specific HIV-1 genetic signature across compartmentalized individuals is strong evidence that the viral quasi-species adapts to the local fitness landscape within the CNS and, moreover, that commonalities in this selective environment exist across individuals. Position 308 (V3 loop position 13) was the most informative sequence position, underscored by the overrepresentation of proline and histidine at this position in the publicly available CSF-derived sequence data. The presence of other residues besides proline and histidine at this site in CSF-derived sequences may result from the contribution of virus from peripheral sources to CSF populations (Ellis *et al.*, 2000). The role of position 308 in HIV-1 neurotropism is highlighted by its discordant entropy scores in CSF and plasma and by the fact that it has been featured in the reports of several independent studies over the last decade (Korber *et al.*, 1994; Power *et al.*, 1994). In addition, the presence of certain residues at position 308 has been associated with macrophage tropism, which is most likely correlated with microglial tropism due to the extensive similarities between these cell types (Chesebro *et al.*, 1996). Understanding the relevance of this sequence position to neurotropism and neuropathogenesis may be achieved by infecting *in vitro* foetal brain aggregates (Trillo-Pazos *et al.*, 2004) or microglial cell cultures with genetically defined HIV-1 strains to determine the fitness consequences associated with p308 polymorphisms.

Our exploration of the relationship between cognitive deficit in the host and viral genetics suggests that V3 loop sequence may be a genetic determinant of neurovirulence.

The contribution of V3 loop position 5 to neurovirulence may result from accelerated pathogenesis due to improved replicative capacity within the CNS (Ellis *et al.*, 1997). However, HIV-1 neurotropism and neurovirulence may be distinct and separable phenomena (Power *et al.*, 1995). Although certain Env mutations may not enhance the replication kinetics of HIV-1 within the CNS, they may increase gp160-mediated neurotoxicity due to alterations in interactions between virion surface glycoproteins and host cell surface molecules (Lipton, 1992; Toggas *et al.*, 1994; Kanmogne *et al.*, 2002). Several investigators have presented evidence that residues elsewhere within the V3 loop may influence HIV neuropathogenesis (Power *et al.*, 1994; Kuiken *et al.*, 1995; Power *et al.*, 1995). These data, taken together, suggest that there may be multiple, independent sequence pathways leading to HIV neurovirulence. Moreover, the extent of variation observed in subtype B V3 loop sequence is not observed in many other clades like subtype C; therefore, the degree of neurotropism and neurovirulence associated with non-B subtypes may differ, as well as their genetic determinants.

There are limitations of this analysis as a result of the specific clinical characteristics of the cohort studied. While the cohort had a wide range of current $CD4^+$ counts (16–688), most had experienced advanced immunosuppression (CD4 nadir < 200) and were partially immune reconstituted on ART. Thus, our results may not be generalizable to individuals with less advanced disease or those who have never seen effective antiretroviral therapy. Additionally, the cases were selected on the basis of having detectable CSF HIV RNA levels, and therefore these results may not be representative of individuals with undetectable CSF viral loads.

The CNS has been characterized as a reservoir, a compartment and a drug sanctuary (Foudraine *et al.*, 1998; Gunthard *et al.*, 2001). Our investigations characterize the differing selection pressures between the CSF and blood and document a specific genetic signature of virus compartmentalized in the CNS. These data offer important insights into the adaptation of HIV to the CNS environment, which may prove valuable in managing HIV-1 infection and preventing the development of neurological disorders.

Supplementary material
Supplementary data are available at *Brain* Online.

Acknowledgements

References
Adachi A, Gendelman HE, Koenig S, Folks T, Willey R, Rabson A, et al. Production of acquired immunodeficiency syndrome-associated retrovirus in human and non-human cells transfected with an infectious molecular clone. J Virol 1986; 59: 284–91.

Argyris EG, Acheampong E, Nunnari G, Mukhtar M, Williams KJ, Pomerantz RJ. Human immunodeficiency virus type 1 enters primary human brain microvascular endothelial cells by a mechanism involving cell surface proteoglycans independent of lipid rafts. J Virol 2003; 77: 12140–51.

Burdo TH, Nonnemacher M, Irish BP, Choi CH, Krebs FC, Gartner S, et al. High-affinity interaction between HIV-1 Vpr and specific sequences that span the C/EBP and adjacent NF-kappaB sites within the HIV-1 LTR correlate with HIV-1-associated dementia. DNA Cell Biol 2004; 23: 261–9.

Carey CL, Woods SP, Gonzalez R, Conover E, Marcotte TD, Grant I, et al. Predictive validity of global deficit scores in detecting neuropsychological impairment in HIV infection. J Clin Exp Neuropsychol 2004; 26: 307–19.

Chesebro B, Wehrly K, Nishio J, Perryman S. Mapping of independent V3 envelope determinants of human immunodeficiency virus type 1 macrophage tropism and syncytium formation in lymphocytes. J Virol 1996; 70: 9055–9.

Chohan B, Lang D, Sagar M, Korber B, Lavreys L, Richardson B, et al. Selection for human immunodeficiency virus type 1 envelope glycosylation variants with shorter V1-V2 loop sequences occurs during transmission of certain genetic subtypes and may impact viral RNA levels. J Virol 2005; 79: 6528–31.

Cinque P, Bossolasco S, Lundkvist A. Molecular analysis of cerebrospinal fluid in viral diseases of the central nervous system. J Clin Virol 2003; 26: 1–28.

Clements JE, Babas T, Mankowski JL, Suryanarayana K, Piatak M Jr, Tarwater PM, et al. The central nervous system as a reservoir for simian immunodeficiency virus (SIV): steady-state levels of SIV DNA in brain from acute through asymptomatic infection. J Infect Dis 2002; 186: 905–13.

Cunningham PH, Smith DG, Satchell C, Cooper DA, Brew B. Evidence for independent development of resistance to HIV-1 reverse transcriptase inhibitors in the cerebrospinal fluid. AIDS 2000; 14: 1949–54.

Dayhoff MO, Schwartz RM, Orcutt BC. A model of evolutionary change in proteins. In: Dayhoff MO, editor. Atlas of Protein Sequence and Structure. Washington, D.C.: National Biomedical Research Foundation; 1978. p. 345–52.

Derdeyn CA, Decker JM, Bibollet-Ruche F, Mokili JL, Muldoon M, Denham SA, et al. Envelope-constrained neutralization-sensitive HIV-1 after heterosexual transmission. Science 2004; 303: 2019–22.

Ellis RJ, Hsia K, Spector SA, Nelson JA, Heaton RK, Wallace MR, et al. Cerebrospinal fluid human immunodeficiency virus type 1 RNA levels are elevated in neurocognitively impaired individuals with acquired immunodeficiency syndrome. HIV Neurobehavioral Research Center Group. Ann Neurol 1997; 42: 679–88.

Ellis RJ, Gamst AC, Capparelli E, Spector SA, Hsia K, Wolfson T, et al. Cerebrospinal fluid HIV RNA originates from both local CNS and systemic sources. Neurology 2000; 54: 927–36.

Felsenstein J. PHYLIP (Phylogeny Inference Package) version 3.5c. Seattle: University of Washington; 1993.

Foudraine NA, Hoetelmans RM, Lange JM, de Wolf F, van Benthem BH, Maas JJ, et al. Cerebrospinal-fluid HIV-1 RNA and drug concentrations after treatment with lamivudine plus zidovudine or stavudine. Lancet 1998; 351: 1547–51.

Gartner S, Markovits P, Markovitz DM, Kaplan MH, Gallo RC, Popovic M. The role of mononuclear phagocytes in HTLV-III/LAV infection. Science 1986; 233: 215–9.

Gonzalez-Scarano F, Martin-Garcia J. The neuropathogenesis of AIDS. Nat Rev Immunol 2005; 5: 69–81.

Gorry PR, Bristol G, Zack JA, Ritola K, Swanstrom R, Birch CJ, et al. Macrophage tropism of human immunodeficiency virus type 1 isolates from brain and lymphoid tissues predicts neurotropism independent of coreceptor specificity. J Virol 2001; 75: 10073–89.

Goudsmit J, Epstein LG, Paul DA, van der Helm HJ, Dawson GJ, Asher DM, et al. Intra-blood-brain barrier synthesis of human immunodeficiency virus antigen and antibody in humans and chimpanzees. Proc Natl Acad Sci USA 1987; 84: 3876–80.

Grant I, Atkinson JH, Hesselink JR, Kennedy CJ, Richman DD, Spector SA, et al. Evidence for early central nervous system involvement in the acquired immunodeficiency syndrome (AIDS) and other human immunodeficiency virus (HIV) infections. Ann Intern Med 1987; 107: 828–36.

Gunthard HF, Havlir DV, Fiscus S, Zhang ZQ, Eron J, Mellors J, et al. Residual human immunodeficiency virus (HIV) Type 1 RNA and DNA in lymph nodes and HIV RNA in genital secretions and in cerebrospinal fluid after suppression of viremia for 2 years. J Infect Dis 2001; 183: 1318–27.

Heaton RK, Grant I, Butters N, White DA, Kirson D, Atkinson JH, et al. The HNRC 500—neuropsychology of HIV infection at different disease stages. HIV Neurobehavioral Research Center. J Int Neuropsychol Soc 1995; 1: 231–51.

Ho DD, Rota TR, Schooley RT, Kaplan JC, Allan JD, Groopman JE, et al. Isolation of HTLV-III from cerebrospinal fluid and neural tissues of patients with neurologic syndromes related to the acquired immunodeficiency syndrome. N Engl J Med 1985; 313: 1493–7.

Hogan TH, Stauff DL, Krebs FC, Gartner S, Quiterio SJ, Wigdahl B. Structural and functional evolution of human immunodeficiency virus type 1 long terminal repeat CCAAT/enhancer binding protein sites and their use as molecular markers for central nervous system disease progression. J Neurovirol 2003; 9: 55–68.

Hudson RR, Slatkin M, Maddison WP. Estimation of levels of gene flow from DNA sequence data. Genetics 1992; 132: 583–9.

Hughes ES, Bell JE, Simmonds P. Investigation of the dynamics of the spread of human immunodeficiency virus to brain and other tissues by evolutionary analysis of sequences from the p17gag and env genes. J Virol 1997; 71: 1272–80.

Kanmogne GD, Kennedy RC, Grammas P. HIV-1 gp120 proteins and gp160 peptides are toxic to brain endothelial cells and neurons: possible pathway for HIV entry into the brain and HIV-associated dementia. J Neuropathol Exp Neurol 2002; 61: 992–1000.

Korber BTM, Kunstman KJ, Patterson BK, Furtado M, McEvilly MM, Levy R, et al. Genetic differences between blood- and brain-derived viral sequences from human immunodeficiency virus type 1-infected patients: evidence of conserved elements in the V3 region of the envelope protein of brain-derived sequences. J Virol 1994; 68: 7467–81.

Kosakovsky Pond SL, Frost SD. Not so different after all: a comparison of methods for detecting amino acid sites under selection. Mol Biol Evol 2005; 22: 1208–22.

Kosakovsky Pond SL, Frost S, Grossman Z, Gravenor M, Richman DD, Leigh Brown A. Adaptation to different human populations by HIV-1 revealed by codon-based analysis. PLoS Comput Biol 2006 (in press).

Koyanagi Y, Miles S, Mitsuyasu R, Merrill JE, Vinters HV, Chen ISY. Dual infection of the central nervous system by AIDS viruses with distinct cellular tropisms. Science 1987; 236: 819–22.

Kuiken CL, Goudsmit J, Weiller GF, Armstrong JS, Hartman S, Portegies P, et al. Differences in human immunodeficiency virus type 1 V3 sequences from patients with and without AIDS dementia complex. J Gen Virol 1995; 76: 175–80.

Leigh Brown AJ. Analysis of HIV-1 *env* gene sequences reveals evidence for a low effective number in the viral population. Proc Natl Acad Sci USA 1997; 94: 1862–5.

Lipton SA. Requirement for macrophages in neuronal injury induced by HIV envelope protein gp120. Neuroreport 1992; 3: 913–5.

Ljunggren K, Chiodi F, Broliden PA, Albert J, Norkrans G, Hagberg L, et al. HIV-1-specific antibodies in cerebrospinal fluid mediate cellular cytotoxicity and neutralization. AIDS Res Hum Retroviruses 1989; 5: 629–38.

Marshall RD. The nature and metabolism of the carbohydrate-peptide linkages of glycoproteins. Biochem Soc Symp 1974; 40: 17–26.

McArthur JC, Haughey N, Gartner S, Conant K, Pardo C, Nath A, et al. Human immunodeficiency virus-associated dementia: an evolving disease. J Neurovirol 2003; 9: 205–21.

McCrossan M, Marsden M, Carnie FW, Minnis S, Hansoti B, Anthony IC, et al. An immune control model for viral replication in the CNS during presymptomatic HIV infection. Brain 2006; 129: 503–16.

Misra A, Ganesh S, Shahiwala A, Shah SP. Drug delivery to the central nervous system: a review. J Pharm Pharm Sci 2003; 6: 252–73.

Nei M, Gojobori T. Simple methods for estimating the numbers of synonymous and nonsynonymous nucleotide substitutions. Mol Biol Evol 1986; 3: 418–26.

Nickle DC, Jensen MA, Shriner D, Brodie SJ, Frenkel LM, Mittler JE, et al. Evolutionary indicators of human immunodeficiency virus type 1 reservoirs and compartments. J Virol 2003a; 77: 5540–6.

Nickle DC, Shriner D, Mittler JE, Frenkel LM, Mullins JI. Importance and detection of virus reservoirs and compartments of HIV infection. Curr Opin Microbiol 2003b; 6: 410–6.

Ohagen A, Devitt A, Kunstman KJ, Gorry PR, Rose PP, Korber B, et al. Genetic and functional analysis of full-length human immunodeficiency virus type 1 env genes derived from brain and blood of patients with AIDS. J Virol 2003; 77: 12336–45.

Olsen GJ, Matsuda H, Hagstrom R, Overbeek R. fastDNAmL: a tool for construction of phylogenetic trees of DNA sequences using maximum likelihood. Comput Appl Biosci 1994; 10: 41–8.

Pachter JS, de Vries HE, Fabry Z. The blood-brain barrier and its role in immune privilege in the central nervous system. J Neuropathol Exp Neurol 2003; 62: 593–604.

Page RD. TreeView: an application to display phylogenetic trees on personal computers. Comput Appl Biosci 1996; 12: 357–8.

Pierson T, McArthur J, Siliciano RF. Reservoirs for HIV-1: mechanisms for viral persistence in the presence of antiviral immune responses and antiretroviral therapy. Annu Rev Immunol 2000; 18: 665–708.

Pillai S, Good B, Richman D, Corbeil J. A new perspective on V3 phenotype prediction. AIDS Res Hum Retroviruses 2003; 19: 145–9.

Pillai SK, Good B, Pond SK, Wong JK, Strain MC, Richman DD, et al. Semen-specific genetic characteristics of human immunodeficiency virus type 1 env. J Virol 2005; 79: 1734–42.

Power C, McArthur JC, Johnson RT, Griffin DE, Glass JD, Perryman S, et al. Demented and nondemented patients with AIDS differ in brain-derived human immunodeficiency virus type 1 envelope sequences. J Virol 1994; 68: 4643–9.

Power C, McArthur JC, Johnson RT, Griffin DE, Glass JD, Dewey R, et al. Distinct HIV-1 env sequences are associated with neurotropism and neurovirulence. Curr Top Microbiol Immunol 1995; 202: 89–104.

Price RW. Neurological complications of HIV infection. Lancet 1996; 348: 445–52.

Quinlan JR. Programs for machine learning. San Francisco: Morgan Kaufmann; 1993.

Rambaut A. Se-Al: Sequence Alignment Editor version 2.0; 1996. Available at http://evolve.zoo.ox.ac.uk/.

Richman DD, Wrin T, Little SJ, Petropoulos CJ. Rapid evolution of the neutralizing antibody response to HIV type 1 infection. Proc Natl Acad Sci USA 2003; 100: 4144–9.

Ross HL, Gartner S, McArthur JC, Corboy JR, McAllister JJ, Millhouse S, et al. HIV-1 LTR C/EBP binding site sequence configurations preferentially encountered in brain lead to enhanced C/EBP factor binding and increased LTR-specific activity. J Neurovirol 2001; 7: 235–49.

Ruta SM, Matusa R, Cernescu CC. Cerebrospinal fluid western blot profiles in the evolution of HIV-1 pediatric encephalopathy. Rom J Virol 1998; 49: 61–71.

Sanjuan R, Codoner FM, Moya A, Elena SF. Natural selection and the organ-specific differentiation of HIV-1 V3 hypervariable region. Evolution Int J Org Evolution 2004; 58: 1185–94.

Shieh JT, Albright AV, Sharron M, Gartner S, Strizki J, Doms RW, et al. Chemokine receptor utilization by human immunodeficiency virus type 1 isolates that replicate in microglia. J Virol 1998; 72: 4243–9.

Slatkin M, Maddison WP. A cladistic measure of gene flow inferred from the phylogenies of alleles. Genetics 1989; 123: 603–13.

Smit TK, Brew BJ, Tourtellotte W, Morgello S, Gelman BB, Saksena NK. Independent evolution of human immunodeficiency virus (HIV) drug resistance mutations in diverse areas of the brain in HIV-infected patients, with and without dementia, on antiretroviral treatment. J Virol 2004; 78: 10133–48.

Song B, Cayabyab M, Phan N, Wang L, Axthelm MK, Letvin NL, et al. Neutralization sensitivity of a simian-human immunodeficiency virus (SHIV-HXBc2P 3.2N) isolated from an infected rhesus macaque with neurological disease. Virology 2004; 322: 168–81.

Staprans S, Marlowe N, Glidden D, Novakovic-Agopian T, Grant RM, Heyes M, et al. Time course of cerebrospinal fluid responses to antiretroviral therapy: evidence for variable compartmentalization of infection. AIDS 1999; 13: 1051–61.

Strain MC, Letendre S, Pillai SK, Russell T, Ignacio CC, Gunthard HF, et al. Genetic composition of human immunodeficiency virus type 1 in cerebrospinal fluid and blood without treatment and during failing antiretroviral therapy. J Virol 2005; 79: 1772–88.

Thompson JD, Higgins DG, Gibson TJ. CLUSTAL W: improving the sensitivity of progressive multiple sequence alignment through sequence weighting, position-specific gap penalties and weight matrix choice. Nucleic Acids Res 1994; 22: 4673–80.

Toggas SM, Masliah E, Rockenstein EM, Rall GF, Abraham CR, Mucke L. Central nervous system damage produced by expression of the HIV-1 coat protein gp120 in transgenic mice. Nature 1994; 367: 188–93.

Trillo-Pazos G, Kandanearatchi A, Eyeson J, King D, Vyakarnam A, Everall IP. Infection of stationary human brain aggregates with HIV-1 SF162 and IIIB results in transient neuronal damage and neurotoxicity. Neuropathol Appl Neurobiol 2004; 30: 136–47.

Venturi G, Catucci M, Romano L, Corsi P, Leoncini F, Valensin PE, et al. Antiretroviral resistance mutations in HIV-1 RT and protease from paired CSF and plasma samples. J Infect Dis 2000; 181: 740–5.

von Gegerfelt A, Chiodi F, Keys B, Norkrans G, Hagberg L, Fenyo EM, et al. Lack of autologous neutralizing antibodies in the cerebrospinal fluid of HIV-1 infected individuals. AIDS Res Hum Retroviruses 1992; 8: 1133–8.

Wei X, Decker JM, Wang S, Hui H, Kappes JC, Wu X, et al. Antibody neutralization and escape by HIV-1. Nature 2003; 422: 307–12.

Witten IH, Frank E. Data mining: practical machine learning tools and techniques with java implementations. San Francisco: Morgan Kaufmann; 2000.

Wong JK, Ignacio CC, Torriani F, Havlir D, Fitch NJ, Richman DD. In vivo compartmentalization of human immunodeficiency virus: evidence from the examination of pol sequences from autopsy tissues. J Virol 1997; 71: 2059–71.

Zhou N, Zhang X, Fan X, Argyris E, Fang J, Acheampong E, et al. The N-terminal domain of APJ, a CNS-based coreceptor for HIV-1, is essential for its receptor function and coreceptor activity. Virology 2003; 317: 84–94.

Zink MC, Suryanarayana K, Mankowski JL, Shen A, Piatak M Jr, Spelman JP, et al. High viral load in the cerebrospinal fluid and brain correlates with severity of simian immunodeficiency virus encephalitis. J Virol 1999; 73: 10480–8.